Synergetic effect of triglycine sulfate and graphite nanoplatelets on dielectric and piezoelectric properties of epoxy resin composites

A. Plyushch[1], J. Macutkevic[1], V. Samulionis[1], J. Banys[1], Dz. Bychanok[2], P. Kuzhir[2,3], S. Mathieu[4], V. Fierro[5], A. Celzard[5]

1. Faculty of Physics, Vilnius University, Sauletekio 9, Vilnius LT-10222, Lithuania

2.Research Institute for Nuclear problems of Belarusian State University, Bobruiskaya Str., 11 Minsk 220030 Belarus

3.Tomsk **State** University, **36**, Lenin ave, Tomsk 634050, Russian Federation

4. IJL–UMR Universite de Lorraine–CNRS n° 7198, 2 allée André Guinier, BP 50840, 54011 Nancy cedex, France

5. IJL–UMR Universite de Lorraine–CNRS, n° 7198, ENSTIB, 27 Rue Philippe Séguin, BP 21042, 88051, Epinal Cedex 9, France

Epoxy resin composites with 30 wt. % of triglycine sulfate (TGS) and up to 1 wt. % of graphite nanoplatelets (GNP) were fabricated and studied by means of broadband dielectric spectroscopy (20 Hz – 3 GHz). It was demonstrated that the dielectric properties are mainly governed by the Maxwell-Wagner relaxation at lower frequencies (below 1 MHz) and by diffuse ferroelectric soft mode at higher frequencies (above 1 MHz). The ferroelectric origin of the phase transitions was also confirmed by piezoelectric investigations. Although the phase transition temperature is independent of GNP concentration, the piezoelectric and dielectric (above 1 MHz) properties of composites are strongly improved by GNP in a broad temperature range. This gives evidence for the strong synergy between GNP and ferroelectric particles. The synergy effect appears due to the better distribution of TGS particles in ternary composites and the creation of electric fields by GNP inside the composite.

1 Introduction

Composite materials based on dielectric polymer matrices filled with different types of conductive inclusions are among the most attracting solids in modern materials science. The main reason is the possibility of improving the properties of the polymer on the one hand, and the quite simple preparation procedure on the other hand. One of the most promising types of inclusions is graphite and its close relatives: carbon nanotubes [1, 2, 3], onion-like carbons [4], and graphite nanoplatelets [5, 6, 7]. When polymer matrices are filled with nanostructured carbon inclusions, the resultant composites demonstrate enhanced dielectric, conductive, thermal and mechanical properties.

On the other hand, composites with ferroelectric inclusions are also widely studied (see [8] and refs. therein). The broad range of possible applications of these materials in microelectronics includes, for example, microwave substrates [9], 3D antennas, embedded capacitors and inductors [10, 11], and electromagnetic shields [12].

Designing ternary composites with carbon and ferroelectric inclusions embedded into polymer matrices is a way to combine the advantages of both fillers [13, 14, 15, 16]. Several authors indeed demonstrated significant improvement of electromagnetic wave absorption properties of such

systems, for instance. Also, the addition of a third phase in nanocarbon / polymer composites may drasticaly change the distribution of carbon particles and, as a result, their dielectric properties. [17, 18]. Even the optimal amount of third phase may be figured out[19].

Triglycine sulfate (TGS) is one of the most well-studied ferroelectric crystal with a second-order ferroelectric phase transition close to 322 K [20]. The ferroelectric phase transition is of order-disorder type with strong dielectric dispersion in the microwave frequency range and a typical critical slowing-down effect [21]. TGS crystals also present huge values of dielectric permittivity, piezoelectric and pyroelectric coefficients, enabling a wide range of applications, including highly sensitive infrared sensors. It is also known that polycrystallinity [22], moisture [23, 24], and doping with either organic or inorganic impurities [25] may significantly affect TGS properties. It is therefore worth investigating the possibility of designing composite materials based on epoxy resin filled with both TGS particles and conductive inclusions. As for the latter, graphite nanoplatelets (GNP) were used. The main ideas are the following: (i) being embedded in epoxy resin, TGS can be protected from ambient moisture; (ii) by introducing various amounts of conductive filler, the dielectric and ultrasonic properties of the composites can be controlled so that polymer composites with improved dielectric and electromagnetic properties can be produced through an easy and cost-effective method.

2 Experimental

2.1 Materials

A single TGS crystal was first dissolved in distilled water. Next, the solution of TGS was evaporated overnight in an oven heated at 90 $^\circ$C. After complete evaporation of water, the solid residue was collected and ground in an agate mortar for 2-3 minutes. As a result, a powder of TGS crystallites was obtained. According to scanning electron microscopy (Fig. 1 (a)), the average size of TGS crystallites was around 50 μm.

GNP particles were obtained by a succession of grinding and sonication steps applied to a suspension of exfoliated graphite in cyclohexane. GNP particles had an average diameter of 10 μm and a typical thickness of 0.1 μm. In other words, their aspect ratio was as high as 100 [26].

2.2 Composites preparation

The composites were prepared as follows. GNP and TGS particles were sonicated in isopropyl alcohol for 3 hours. Next, degassed epoxy resin (Buehler EpoThin 2) was introduced into the solution, and the blend was sonicated for 1 additional hour. The homogeneous solution was then placed into an oven at 60-70 $^\circ$C until complete evaporation of the alcohol. After evaporation, the system was sonicated again for one more hour. When homogenisation was finished, the curing agent was introduced and the obtained system was carefully stirred manually for 5 minutes and poured into the moulds for curing. Composites were cured overnight at room temperature first, than for 5 hours at 80 $^\circ$C.

Based on the aforementioned protocol, samples with either 0 or 30 wt. % of TGS and 0, 0.5, or 1 wt. % of GNP were prepared. Scanning electron microscopy (Fig. 1 (b,c)) demonstrated that both GNP and TGS inclusions were well-dispersed. No percolation paths between TGS crystallites were observed, so the connectivity of the composite may be assumed to be 0-3, since the polymer matrix is interconnected along the 3 directions, while TGS crystallites are not, along any direction. In the following, samples were referred to as wt_{GNP} GNP- wt_{TGS} TGS, where wt means weight percent.

2.3 Broadband dielectric spectroscopy

Dielectric properties of the samples were measured in the frequency range 20 Hz – 1 MHz

with an HP4284A LCR meter. Samples with a typical thickness of 1.2 mm and cross section of 25 mm ^{2} were studied. In the frequency range 1 MHz – 3 GHz, samples were analysed by a coaxial dielectric spectrometer with an Agilent 8714ET vector network analyser. In this case, samples had typical cross section and thickness of 2 mm^2 and 0.3 mm, respectively. Temperature measurements were performed in a home-made furnace, using a heating / cooling rate of 1 K/min. Silver paste was applied for making electrical contacts with the samples.

2.4 Piezoelectric properties

The temperature dependence of piezoelectric sensitivity was investigated by using a pulse-echo ultrasonic setup according to the procedure described elsewhere [27, 28]. A Z-cut $LiNbO_3$ piezoelectric transducer was used for sending 10 MHz ultrasonic waves to a quartz buffer. The ultrasonic waves excited a 0.25 mm-thick composite plate working as a receiving ultrasonic transducer attached to another end of the quartz buffer. The thickness of the composite was close to half of the ultrasonic wavelength in epoxy at 10 MHz frequency. The piezoelectric voltage in the form of 10 MHz radio-pulses was measured by an Agilent DSO3202A digital scope incorporated into the electronic pulse-echo setup for automatic temperature measurements. .

3 Results and Discussion

3.1 Dielectric properties at room temperature

The frequency dependence of the complex dielectric permittivity for all studied composites at room temperature is presented in Fig. 2

As it can be seen from the figure, the addition of either TGS or GNP led to an increase of both real and imaginary parts of the complex dielectric permittivity. In order to understand the influence of the addition of each component on the dielectric properties of composites, the following approach was used. The behaviour of the TGS / epoxy binary system may be predicted by Jayasundere and Smith model of 0-3 composite with dielectric matrix and piezoelectric inclusions [29]. On the other hand, the concentration behaviour of the dielectric properties of GNP / epoxy composites may be described with a simple universal power law, or with the Maxwell-Garnett equation [30]. But in the case of ternary TGS - GNP / epoxy system, the combination of those models might fail at high filler concentrations due to the following reasons. Considering a composite whose total volume is equal to V_0, then the volumes occupied by TGS and GNP particles are is V_{TGS} and $V' = V_0 - V_{TGS}$, respectively. Therefore, the local volume concentration of GNP in the region between TGS particles should be higher than in a binary GNP / epoxy system having the same overall concentration of GNP. The percolation network should thus appear at a comparatively lower weight concentration. On the other hand, TGS crystals may introduce additional barriers preventing contacts between conductive GNP clusters. These two effects are antagonistic so that the final properties of ternary composites should be more sensitive to the microstructure than binary ones.

In the present case, a slight enhancement of dielectric properties was observed for xGNP-30TGS composites with respect to xGNP-0TGS at lower frequencies (below 1 MHz), mainly because: (i) the studied concentration range (0-1 wt. %) of GNP was lower than the percolation threshold [31], (ii) the amount of TGS was quite high, so it is most likely that TGS particles acted as additional barriers in the conductive GNP network.

The dielectric permittivity and dielectric losses strongly decreased with frequency for all composites. Two different dielectric dispersion trends could be distinguished: one at lower frequencies (20 Hz - 1 MHz), where the dielectric permittivity was strongly frequency-dependent, and another one at higher frequencies (above 1 MHz), where dielectric losses were quite low (lower than 1) and the dielectric permittivity was almost frequency-independent.

The dielectric dispersion at lower frequencies can be caused by the dynamics of ferroelectric domains, similarly as in pure TGS crystals, or by the Maxwell-Wagner relaxation due to the high electrical conductivity of GNP, the random orientation of TGS crystallites, and their finite value of electrical conductivity. However, the contribution of ferroelectric domains dynamics should be neglected because the dielectric dispersion remains far above the phase transition temperature. Therefore, the main contribution at low frequencies comes from the Maxwell-Wagner relaxation. It means that the differences in dielectric properties of composites at lower frequencies are mainly related to the structure of conductive clusters.

On the other hand, at higher frequencies at which the impact of GNP on the dielectric permittivity is more significant, the contribution of ferroelectric soft mode, typical of TGS crystals, might also be substantial. In other words, the ferroelectric polarization of TGS clusters may be affected by the presence of GNP because: 1) the distribution of TGS crystallites is better due to the presence of GNP, 2) GNP particles (due to their high electrical conductivity) create electric fields inside the composite, which affect the polarization inside TGS crystallites. Both contributions should be important in the present composites.

3.2 Dielectric properties above room temperature

The maximum of dielectric permittivity close to T=322 K for all studied composites is typical of the ferroelectric transition in pure TGS crystals, except the substantially lower dielectric permittivity peak value due to the random orientation of TGS crystallites (see Fig. 3). The variation of dielectric permittivity near the Curie point T_C reads:

$$\varepsilon' = \frac{C}{|T - T_C|} \tag{1}$$

both in paraelectric and ferroelectric phase (Fig. 3), although with a different value of the constant C. The corresponding parameters of the fits of Eq. (1) are collected in Table 1.

Table 1. Parameters of the fits of Eq. 1 to the data of Fig. 3; C and C' are the constants of Eq. 1 for para- and ferroelectric phases, respectively.

Sample	C', K; ferroelectric phase	C, K; paraelectric phase
0GNP-30TGS	854.24	3235.42
0.5GNP-30TGS	3023.05	4509.23
1GNP-30TGS	2217.91	10428.83

The Curie constants C and C' increased with the GNP concentration, due to the rise of dielectric permittivity. The Curie-Weiss behaviour is usually related to ferroelectric soft mode: either resonant or relaxational [32]. For TGS crystals, the relaxational soft mode is usual [32].

It can also be seen that the addition of GNP did not affect the temperature of the phase transition. However, it increased the absolute value of the complex permittivity in a broad temperature range, especially the real part, while the shape of the curves roughly remained the same. This should be due to the strong synergy effect between TGS particles and GNP. Indeed, the contribution of the Maxwell-Wagner relaxation (which appears at the dielectric / GNP interface) to the dielectric permittivity should not present any anomaly close to the ferroelectric phase transition temperature. Such a contribution should strongly increase with temperature. This was not the case for the composites investigated here.

The temperature dependence of dielectric permittivity of 0.5GNP-30TGS at different

frequencies is shown in Fig. 4. The same typical behaviour was also observed for all investigated composites.

It is clearly seen that at higher frequencies (above 1 MHz), a more pronounced maximum of permittivity appears at a certain intermediate temperature close to 322 K. In contrast, at lower frequencies (below 1 MHz), the dielectric properties are mostly governed by the Maxwell-Wagner relaxation, i.e., are thermally activated and almost not affected by the ferroelectric phase transition.

The frequency dispersion in the high-frequency range (above 1 MHz) can be well described by the universal Jonscher law:

$$\chi(\omega) = \varepsilon(\omega) - \varepsilon_\infty = A(T)(i\omega)^{n(T)-1} \quad (2)$$

where $A(T)$ is a temperature-dependent parameter, and ε_∞ is a suitable "high-frequency" value of the permittivity at which the low-frequency losses become negligible. The exponent $n(T)$ is weakly temperature-dependent and is smaller than unity. This law states that real and imaginary parts of $\chi(\omega)$ have the same frequency dependence:

$$\frac{\chi''(\omega)}{\chi'(\omega)} = cot(\frac{\pi n}{2}) \quad (3)$$

The universal law is associated with many-body interactions between dipoles or charges responsible for polarisation in dielectrics. The parameters of Eq. (3) describing the frequency dependence are collected in Table 2.

Table 2. Parameters of the fits of Eq. 3 to the data of Fig. 5.

Temperature, K	0GNP-30TGS		0.5GNP-30TGS		1GNP-30TGS	
	n	ε_∞	n	ε_∞	n	ε_∞
315	0.92791	3.3	0.81849	8.1	0.74336	9.1
320	0.92083	3.4	0.80642	8.1	0.75913	9
322	0.9177	3.5	0.81328	8.3	0.79987	9
325	0.92083	3.4	0.81328	8.2	0.82416	8.8
330	0.92711	3.1	0.80304	8.1	0.81218	8.7
335	0.9177	3.2	0.8091	8.1	0.81648	8.6
340	0.90521	3.4	0.80059	8.0	0.81788	8.6

It can be seen that the values slightly depended on temperature, especially ε_∞ demonstrated maxima close to the phase transition temperature for all studied samples. However, those values strongly depended on the GNP concentration. Firstly, ε_∞ obviously increased with the concentration, but at the same time, the value of n decreased. This may be explained as follows: below the percolation threshold, the GNP loading made the real part of the permittivity increase faster than the imaginary part.

At lower frequencies the Maxwell-Wagner relaxation of composites takes place. For Maxwell-Wagner relaxations analysis, it is more convenient to use the diectric modulus $M^* = 1/\varepsilon^*$ formalism (see Fig. 6).

The imaginary part of the dielectric modulus demonstrate a maximum at certain frequency. The relaxation times can be calculated as the inverse of the frequency at which the imaginary part of the electrical modulus is the highest, i.e., $\tau = 1/f_{max}$. The variation of the relaxation times at different temperatures was tracked out and the results are presented in Fig. 7.

Such behaviour of the electrical modulus frequency dependence was observed only in ternary

composites. The interfacial polarisation likely occurred at the conductive GNP clusters and TGS interfaces. The relaxation time τ obtained from the electrical modulus is proportional to the resistivity R and to the capacitance of conductive clusters C, i.e., $\tau = RC \propto C/\sigma$. Now, the capacitance only depends on the geometry of the GNP clusters. Assuming a spherical shape, which for GNP is a rough approximation, aimed at capturing the underlying physics, $C = 4\pi\varepsilon_0 r$, where r is an effective radius. Bigger conductive clusters thus lead to lower electrical conductivity and to higher capacitance, and hence to longer relaxation times [33]. Therefore, the biggest clusters are present in composites only containing TGS inclusions, and the smallest ones are in 0.5GNP-30TGS. The Maxwell-Wagner relaxation is related to the onset of conductivity at higher temperatures or higher GNP concentration.

3.3 Piezoelectric properties

Fig. 8 presents measurement results of piezoelectric properties of composite materials.

The temperature dependence of the piezoelectric voltage at 10 MHz frequency exhibited the ferroelectric phase transition at 322 K. Above the transition temperature, the piezoelectric signal of non-polarized samples vanished, but it kept a finite value in the paraelectric phase for the polarised samples. The signal in the paraelectric phase is caused by the electrostriction effect [34]. It can be demonstrated that the detected piezoelectric signal varies with temperature in the same manner as the order parameter η_0 [28, 35].

It was clearly seen that adding GNP provides a strong synergy effect. Composites with only TGS particles indeed did not show piezoelectric response without external polarisation field. Addition of 0.5 wt. % of GNP significantly changed the situation: a weak piezoelectric response appeared even without external electric field. Finally, adding 1 wt. % of GNP provided a strong piezoelectric response without external polarisation. Even more, the difference between responses with and without polarisation decreased when increasing the GNP amount.

Similarly, as in the case of dielectric properties, two possible reasons of this behaviour can be indicated. On the one hand, the loading of GNP obviously impacts the distribution of TGS crystals. Being more homogeneous, composites with TGS and GNP provide the highest piezoelectric response. On the other hand, the addition of GNP might improve the mechanical and electrical properties of epoxy.

Two possible mechanisms of influence of the epoxy properties may be figured out. Firstly, by excitation with ultrasonic waves, the TGS crystals generate charges on their surfaces. The nearby regions thus accumulate the charges. Since the concentration of GNP is quite low (below the percolation threshold), the GNP loading provides a capacitive impact, while conductivity of the samples remains low and appearance of the loss currents is impossible. Due to higher capacitance, the GNP / epoxy composite media which surrounds the TGS crystallites may accumulate electric charges better. The field created by those charges provides additional polarisation of TGS. Thus, the increase of GNP concentration should provide higher piezoelectric response of samples without external polarisation. Secondly, it is known that addition of carbon inclusions improves the mechanical properties of the polymers. Due to that, the ultrasonic waves might propagate throughout with fewer losses than in pure polymers. So, through hardening by GNP addition, composites should present higher piezoelectric properties.

4 Conclusion

Epoxy resin composites with 30 wt. % inclusions of TGS and up to 1 wt. % inclusions of GNP demonstrate ferroelectric properties. The ferroelectric phase transition in these composites was confirmed by the dielectric anomaly and the appearance of piezoelectric properties in the low temperature phase (below the Curie point). The dielectric properties are mainly governed by the

Maxwell-Wagner relaxation (below 1 MHz) and the ferroelectric soft mode (above 1 MHz). Although the ferroelectric phase transition temperature in ternary composites is the same as in pure TGS crystals, GNP and TGS particles demonstrate an evident synergy effect in dielectric and piezoelectric properties. Below their percolation concentration, more GNP nanoparticles lead to an increase of both dielectric permittivity and piezoelectric signals in a broad temperature range. The effect can be explained by a better distribution of particles, an improvement of the mechanical properties, and the creation of internal electric fields by GNP. Therefore, GNP addition should be considered as a relevant and easy way of improving the ferroelectric properties of ternary polymeric composites with ferroelectric and GNP inclusions.

Acknowledgements

The authors acknowledge with thanks the following financial supports: Gilibert PHC exchange project "Dielectric and electric properties of hollow carbon spheres and mesoporous carbon" between France and Lithuania, Nano-Thin and Micro-Sized Carbons: Toward Electromagnetic Compatibility Application, project FP7-610875 NAMICEMC, Multifunctional Graphene-based Nanocomposites with Robust Electromagnetic and Thermal Properties for 3D-printing Application, project H2020 RISE 734164 Graphene 3D. Polina Kuzhir is thankful to Tomsk State University Competitiveness Enhancement Program grant.

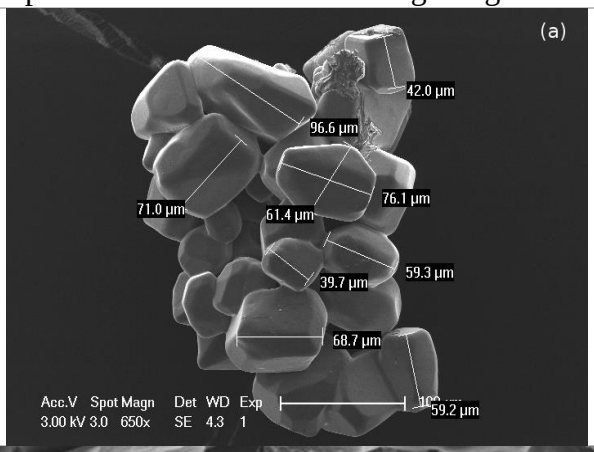

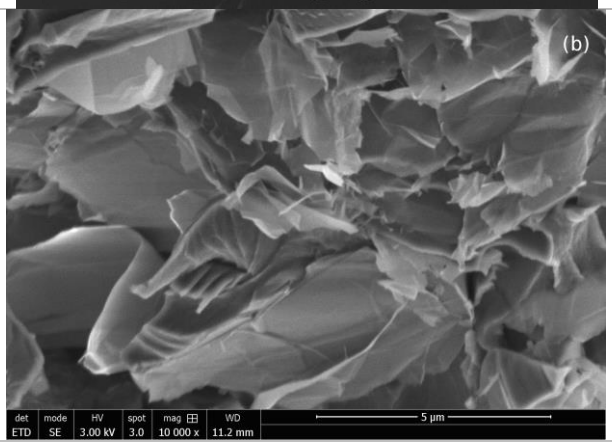

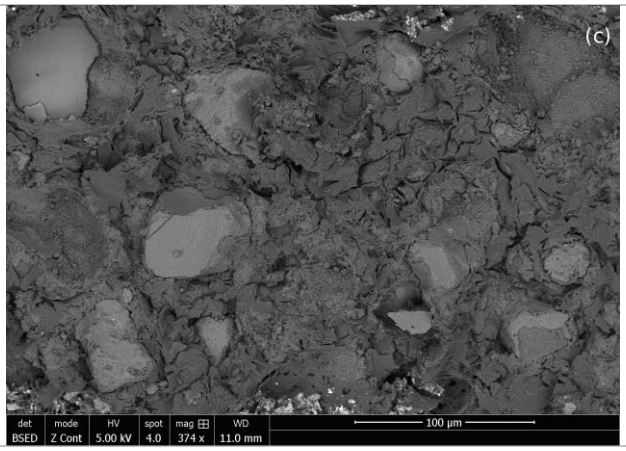

Figure 1: Scanning electron microscopy images of: (a) TGS crystallites; (b) GNP particles; and (c) composite material loaded at 30 and 0.5 wt.% of TGS and GNP, respectively.

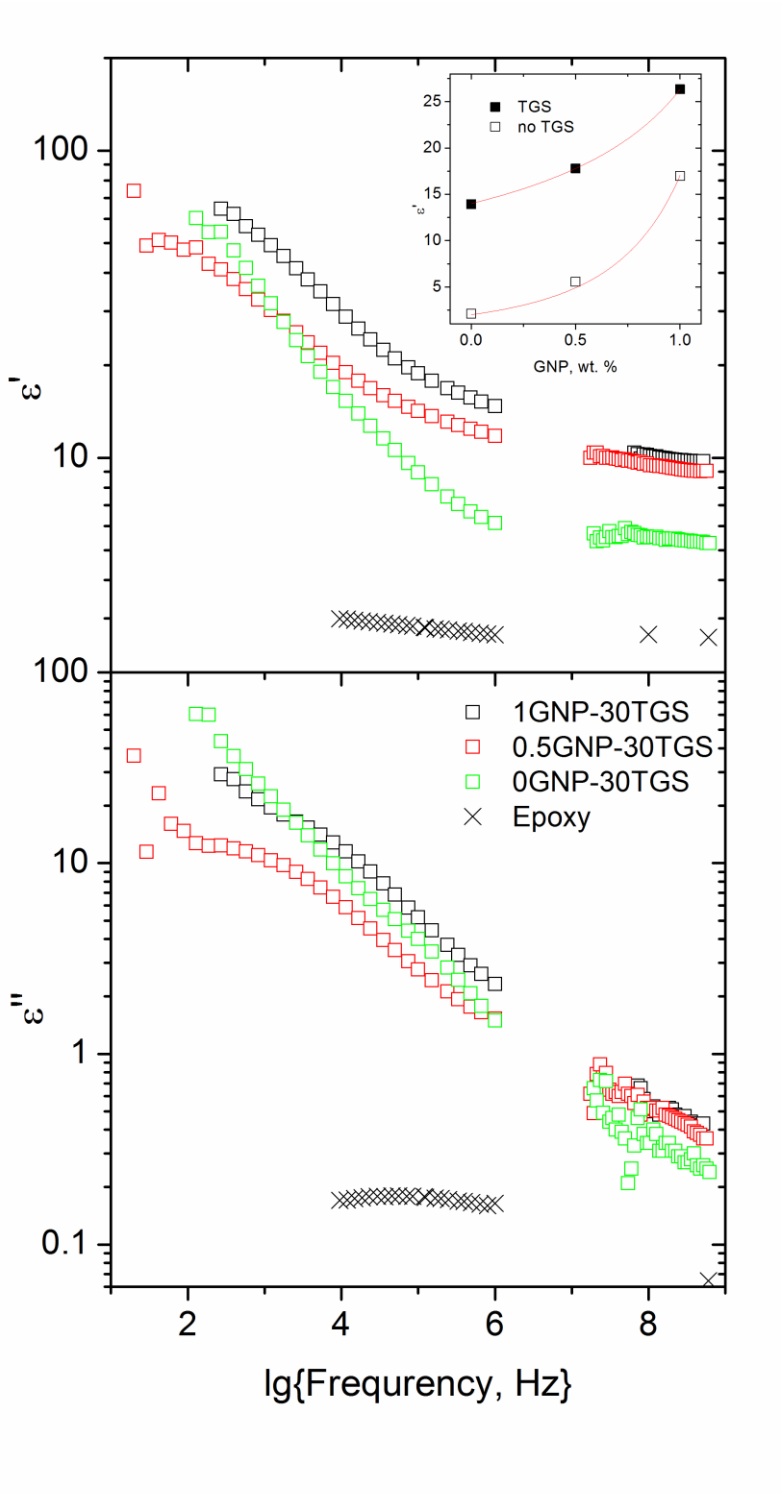

Figure 2: Frequency spectra of dielectric permittivity of pure epoxy and of composite materials filled with 30 wt. % of TGS and different amounts of GNP at room temperature. Inset: comparison of dielectric constant of xGNP-30TGS and xGNP-0TGS at a frequency of 16667 Hz.

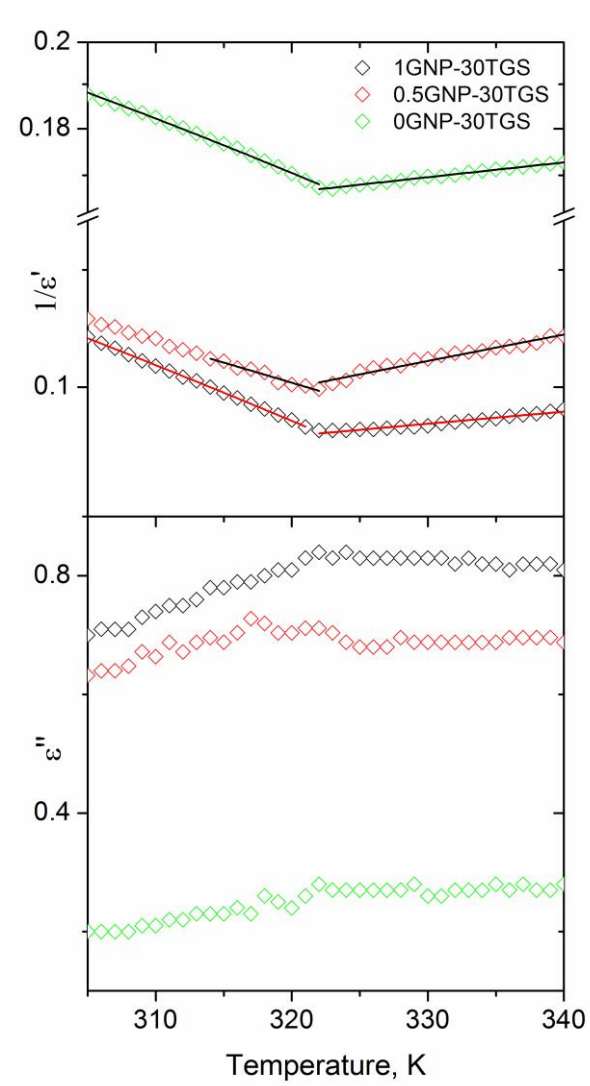

Figure 3: Temperature dependence of the dielectric permittivity of composite materials filled with 30 wt. % of TGS and different amounts of GNP above room temperature, and at frequency 1 GHz. Solid lines are fits with Eq. (1).

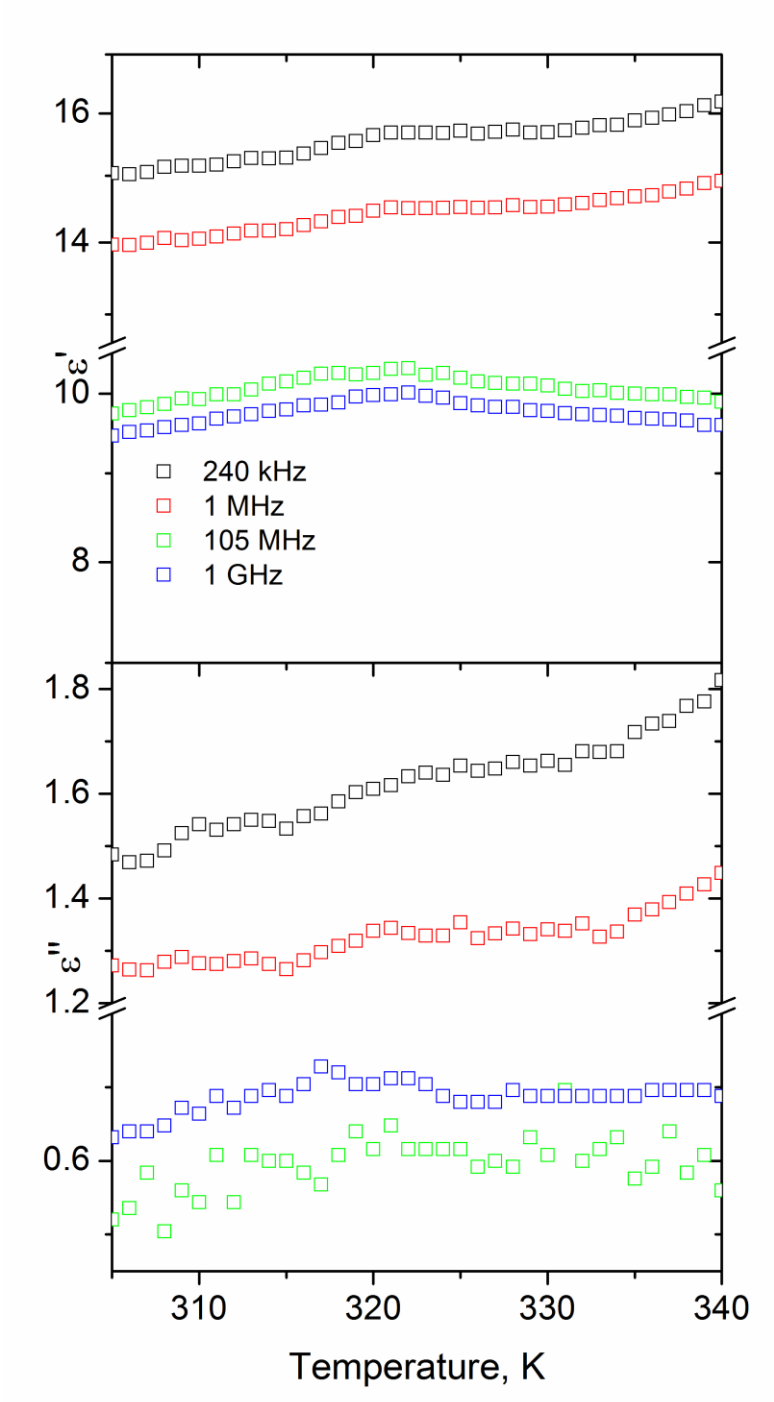

Figure 4: Temperature dependence of the dielectric permittivity of composite materials filled with 30 wt. % of TGS and 0.5 wt. % of GNP at different frequencies.

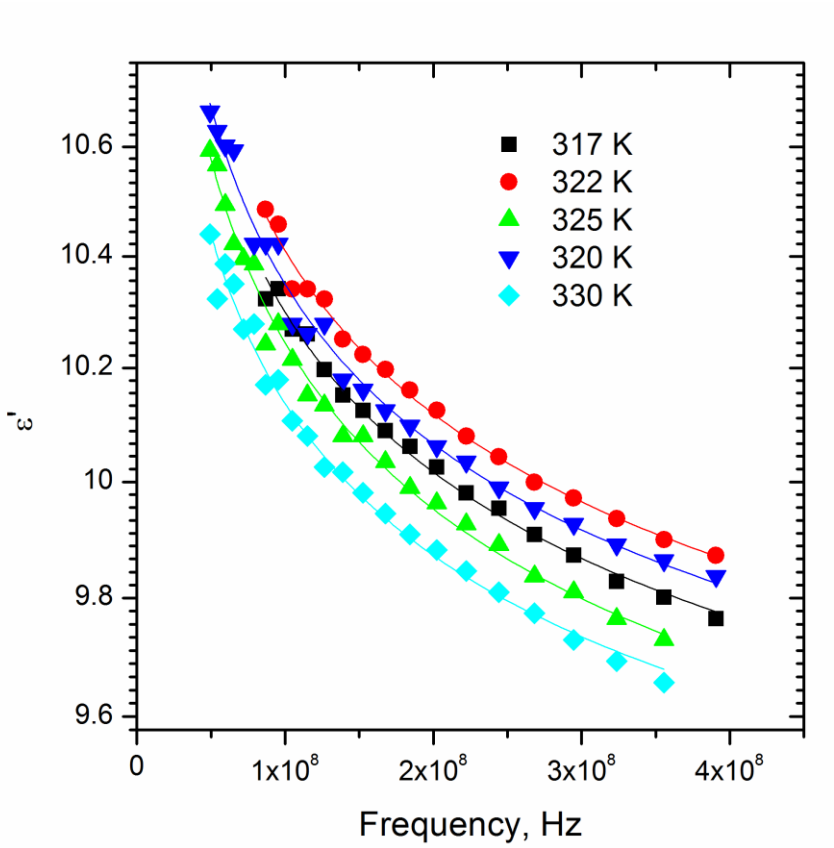

Figure 5: Frequency dependence of the dielectric permittivity of composite materials filled with 30 wt. % of TGS and 0.5 or 1 wt. % of GNP at different temperatures. Solid lines are fits with Eq. (2).

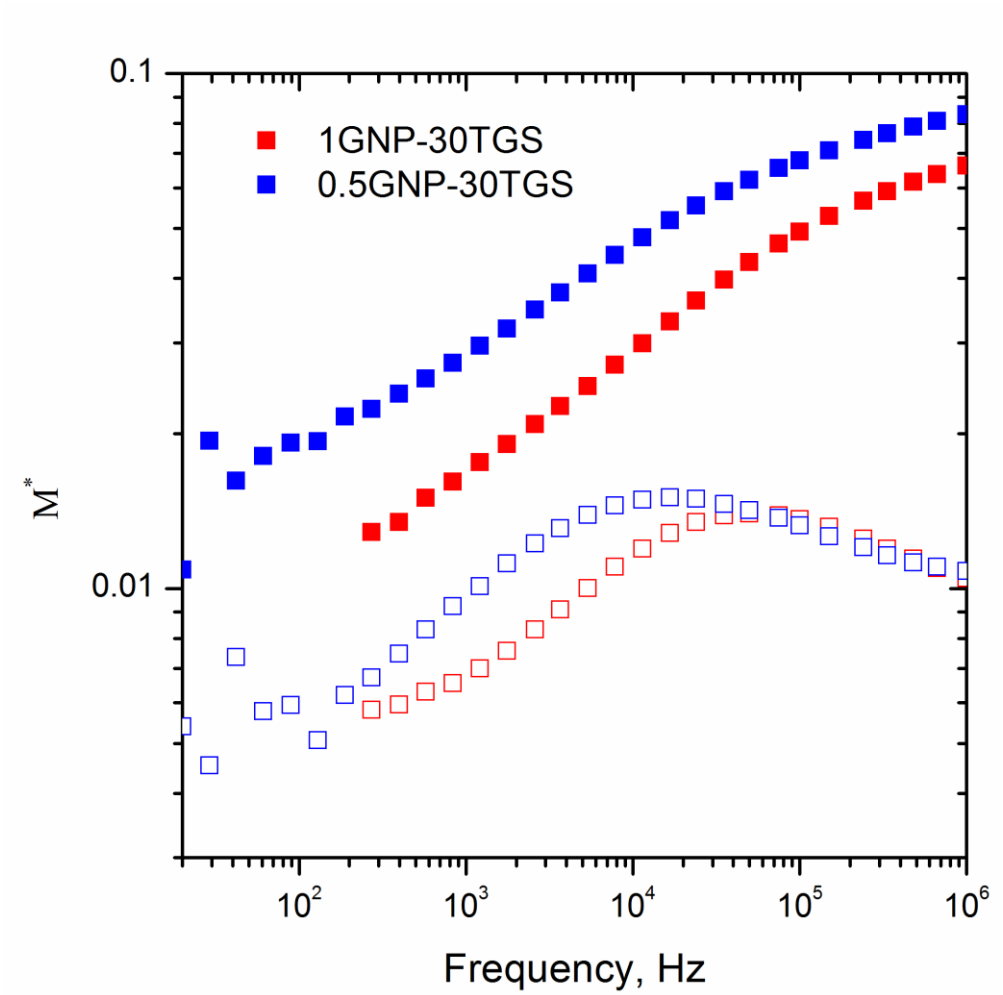

Figure 6: Frequency dependence of the electric modulus of composite materials filled with 30 wt. % of TGS and 0.5 or 1 wt. % of GNP at 300 K. Solid and open symbols are for real and imaginary parts, respectively

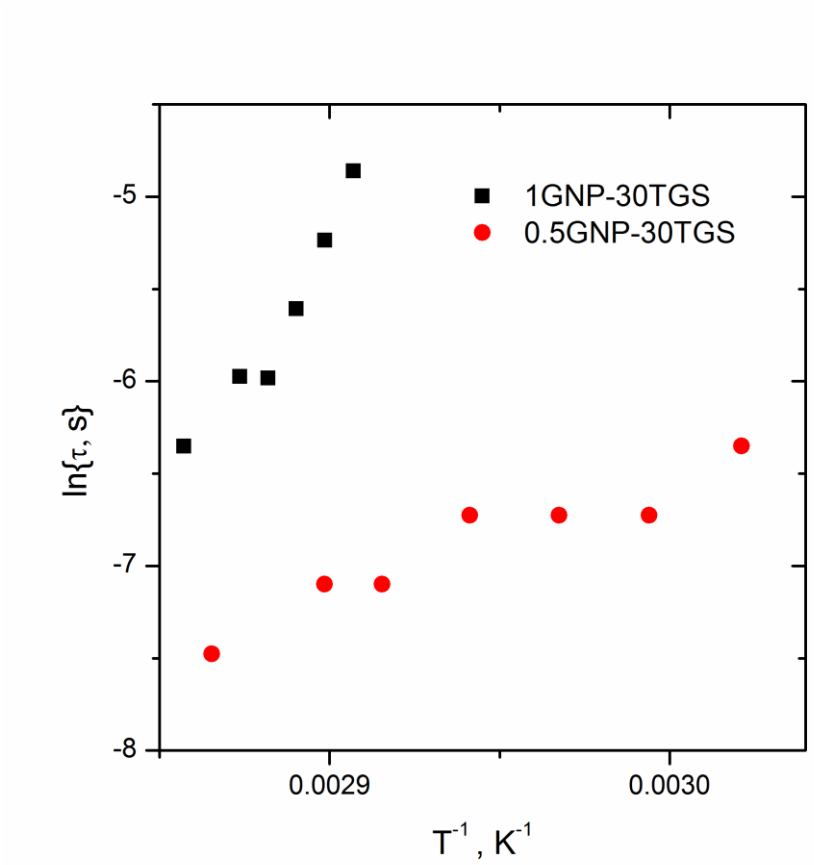

Figure 7: Temperature dependence of the relaxation time for the same ternary composites as in Fig. 6.

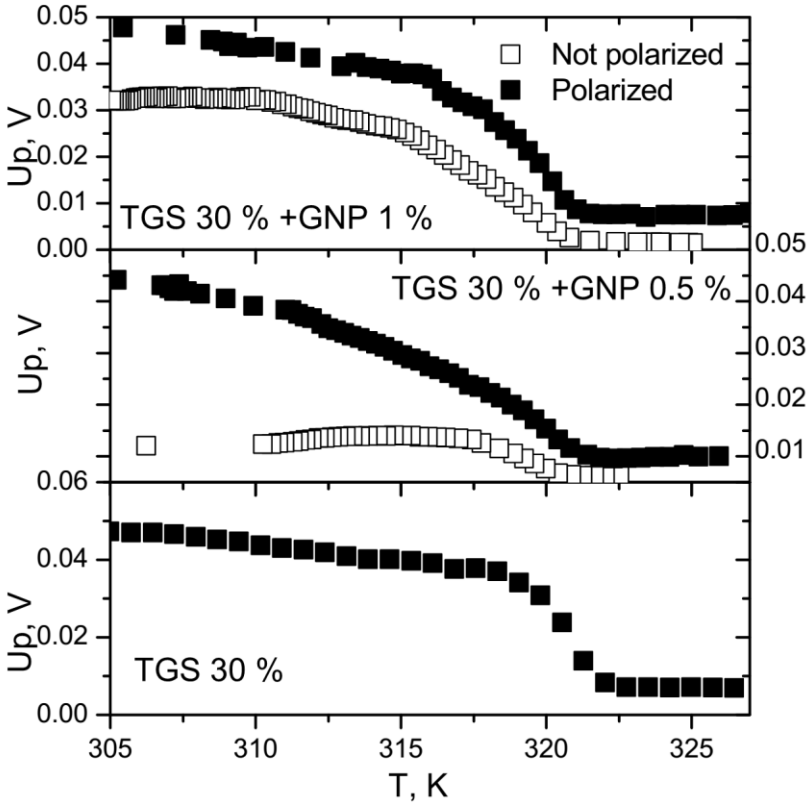

Figure 8: Piezoelectric response of composite materials either polarised with an external field of 400 V/mm (solid symbols) or not polarised (open symbols).

References

[1] P.J. Harris, International Materials Reviews **49**(1), 31 (2004)

[2] E.T. Thostenson, Z. Ren, T.W. Chou, Composites science and technology **61**(13), 1899 (2001)

[3] R.H. Baughman, A.A. Zakhidov, W.A. De Heer, science **297**(5582), 787 (2002)

[4] L. Liu, A. Das, C.M. Megaridis, Carbon **69**, 1 (2014)

[5] B. Li, W.H. Zhong, Journal of materials science **46**(17), 5595 (2011)

[6] A. Yu, P. Ramesh, M.E. Itkis, E. Bekyarova, R.C. Haddon, The Journal of Physical Chemistry C **111**(21), 7565 (2007)

[7] Z. Anwar, A. Kausar, I. Rafique, B. Muhammad, Polymer-Plastics Technology and Engineering **55**(6), 643 (2016)

[8] M.T. Sebastian, H. Jantunen, International Journal of Applied Ceramic Technology **7**(4), 415 (2010)

[9] C. Brosseau, P. Quéffélec, P. Talbot, Journal of Applied Physics **89**(8), 4532 (2001)

[10] S.K. Bhattacharya, R.R. Tummala, Journal of Materials Science: Materials in Electronics **11**(3), 253 (2000)

[11] Q. Wang, L. Zhu, Journal of Polymer Science Part B: Polymer Physics **49**(20), 1421 (2011)

[12] X. Chen, G. Wang, Y. Duan, S. Liu, Journal of Physics D: Applied Physics **40**(6), 1827 (2007)

[13] Z.M. Dang, S.H. Yao, J.K. Yuan, J. Bai, The Journal of Physical Chemistry C **114**(31),

13204 (2010)
[14] K. Piasotski, D. Bychanok, G. Gorokhov, D. Meisak, A. Plyushch, P. Kuzhir, A. Sokol, K. Lapko, A. Sánchez-Sánchez, V. Fierro, et al., Physics, Chemistry and Application of Nanostructures: Reviews and Short Notes to Nanomeeting-2017 p. 202 (2017)
[15] L. Yu, Y. Zhu, C. Qian, Q. Fu, Y. Zhao, Y. Fu, Journal of Nanomaterials **2016** (2016)
[16] B. Luo, X. Wang, E. Tian, H. Gong, Q. Zhao, Z. Shen, Y. Xu, X. Xiao, L. Li, (2016)
[17] H.D. Bao, Z.X. Guo, J. Yu, Polymer **49**(17), 3826 (2008)
[18] Y.F. Lan, J.J. Lin, The Journal of Physical Chemistry A **113**(30), 8654 (2009)
[19] B. De Vivo, P. Lamberti, G. Spinelli, V. Tucci, L. Guadagno, M. Raimondo, L. Vertuccio, V. Vittoria, Composites Science and Technology **89**, 69 (2013)
[20] R. Hill, S. Ichiki, Physical Review **128**(3), 1140 (1962)
[21] R. Blinc, S. Detoni, M. Pintar, Physical Review **124**(4), 1036 (1961)
[22] M. Amin, K. Darwish, S. Ibrahim, Ferroelectrics **76**(1), 33 (1987)
[23] V. Khutorsky, S.B. Lang, Journal of applied physics **82**(3), 1288 (1997)
[24] V. Khutorsky, S. Lang, in *Applications of Ferroelectrics, 1994. ISAF'94., Proceedings of the Ninth IEEE International Symposium on* (IEEE, 1991), pp. 817–820
[25] N.T. Shanthi, P. Selvarajan, C. Mahadevan, Current Applied Physics **9**(5), 1155 (2009)
[26] A. Celzard, E. McRae, J. Mareche, G. Furdin, M. Dufort, C. Deleuze, Journal of Physics and Chemistry of Solids **57**(6-8), 715 (1996)
[27] V. Samulionis, J. Banys, Y. Vysochanskii, Journal of electroceramics **22**(1-3), 192 (2009)
[28] V. Samulionis, J. Banys, Y. Vysochanskii, in *Materials Science Forum*, vol. 636 (Trans Tech Publ, 2010), vol. 636, pp. 398–403
[29] N. Jayasundere, B. Smith, Journal of Applied Physics **73**(5), 2462 (1993)
[30] J.C.M. Garnett, Philosophical Transactions of the Royal Society of London A: Mathematical, Physical and Engineering Sciences **203**(359-371), 385 (1904).
[31] A. Celzard, E. McRae, C. Deleuze, M. Dufort, G. Furdin, J. Marêché, Physical Review B **53**(10), 6209 (1996)
[32] J. Scott, Reviews of Modern Physics **46**(1), 83 (1974)
[33] A. Plyushch, J. Macutkevic, P. Kuzhir, J. Banys, D. Bychanok, P. Lambin, S. Bistarelli, A. Cataldo, F. Micciulla, S. Bellucci, Composites Science and Technology **128**, 75 (2016)
[34] V. Samulionis, J. Banys, Y. Vysochanskii, in *Materials science forum*, vol. 514 (Trans Tech Publ, 2006), vol. 514, pp. 230–234
[35] V. Samulionis, J. Banys, Y. Vysochanskii, Ferroelectrics **379**(1), 69 (2009)